IEICE TRANS. COMMUN., VOL. E77-B, NO. 1 JANUARY 1994

PAPER

Fundamental Study on Synthetic Aperture FM-CW Radar Polarimetry

Yoshio YAMAGUCHI†, *Member*, Toru NISHIKAWA†, *Associate Member*, Masakazu SENGOKU†, Wolfgang-M. BOERNER††, *and* Hyo Joon EOM,††† *Members*

SUMMARY This paper applies the principle of radar polarimetry to the synthetic aperture frequency modulated continuous wave radar. First, the principle of monochromatic wave radar polarimetry using scattering matrix and polarization ratio necessary for introducing polarimetric imaging is given. In order to accommodate this principle to a wideband radar, a scattering matrix must be introduced, because FM-CW radar utilizes a wideband signal. This paper points out that the polarimetric target reflection coefficient obtained by the synthetic aperture FM-CW radar works as the scattering matrix element. This replacement, i.e., polarimetric reflection coefficient = the scattering matrix element, was verified by an experiment based on the polarization ratio which maximizes and minimizes a target. A radar system operative in the microwave X-band was successfully applied to the polarimetric detection of a metallic pipe of different orientations, demonstrating the validity of FM-CW radar polarimetry, and indicating an establishment of full polarimetric radar system.

key words: *measurement and metrology, radio applications, radar*

1. Introduction

Radar polarimetry, i.e., the full utilization of vector nature of electromagnetic wave information, has become an indispensable tool in advanced radar systems. The principle of radar polarimetry for monochromatic (single frequency) wave has already been established by many investigators [1]–[7]. However, the wideband polarimetry is still in the developmental phase. Since we have been dealing with a wideband FM-CW radar [8], the problem is how to introduce the radar polarimetry into this radar system.

In this paper, we regarded the polarimetric target reflection coefficient obtained by a synthetic aperture FM-CW radar as the element of scattering matrix in order to introduce the polarimetry. Although the coefficient is derived from a wideband signal, it is a single complex value, and we regard it represents target scattering information, provided that the scattering characteristics are almost constant under the bandwidth. The polarimetric measurement provides full scattering matrix elements. If the replacement, i.e., target reflection coefficient = scattering matrix element, is possible, then the polarization synthesis (optimal power reception) should work well in detection or imaging problems. Therefore, the main purpose of the paper is to confirm the validity of the replacement. If the validity is confirmed, it leads to an establishment of full polarimetric synthetic aperture radar system.

In the following, the principle of radar polarimetry for the monochromatic wave is given, which is the basis for polarimetric detection and imaging. The principle of synthetic aperture FM-CW radar is outlined in Sect. 3 indicating that a target reflection coefficient can be replaced by a scattering matrix element. Section 4 shows an experimental verification. A radar system operative in the microwave X-band was applied to the polarimetric detection of a metallic pipe of different orientations using a phase calibration technique. It is shown that the polarimetry can be applied to the FM-CW radar.

2. Principle of Polarimetric Imaging with Scattering Matrix and Polarization Ratio

In this section, the rigorous principle of radar polarimetry necessary for introducing polarimetric imaging is given. In the polarization basis (AB) with unit vectors $\hat{\boldsymbol{A}}$ and $\hat{\boldsymbol{B}}$, the electric field vector of a time harmonic plane wave can be expressed in the transverse plane as

$$\boldsymbol{E}(AB)=E_A\hat{\boldsymbol{A}}+E_B\hat{\boldsymbol{B}} \tag{1}$$

The polarization ratio in this basis is defined as

$$\rho_{AB}=\frac{E_B}{E_A}=\frac{|E_B|}{|E_A|}\,e^{j(\phi_B-\phi_A)}=|\rho_{AB}|e^{j\phi_{AB}} \tag{2}$$

where $\phi_{AB}=\phi_B-\phi_A$ is the phase difference. Using this polarization ratio and assuming that the magnitude of the electric vector is unity, the wave can be written in

Manuscript received May 19, 1993.
Manuscript revised August 5, 1993.

† The authors are with the Faculty of Engineering, Niigata University, Niigata-shi, 950-21 Japan.
†† The author is with the Department of Electrical Engineering and Computer Science, University of Illinois at Chicago, Chicago, IL 60607-7018 USA.
††† The author is with the Department of Electrical Engineering, Korea Advanced Institute of Science and Technology, Teajon, 305-701 Korea.

the Jones vector form as

$$E(AB)=\frac{1}{\sqrt{1+\rho_{AB}\rho_{AB}^{*}}}\begin{bmatrix}1\\ \rho_{AB}\end{bmatrix} \tag{3}$$

Now, let $\boldsymbol{E}_t$ be the transmitted wave from a radar, and $\boldsymbol{E}_s$ be the scattered wave from a target arriving at the receiver. The scattered wave can be related to the transmitted wave via scattering matrix $[S]$.

$$\begin{aligned}\boldsymbol{E}_s(AB)&=\begin{bmatrix}E_s^A\\ E_s^B\end{bmatrix}\\ &=\begin{bmatrix}S_{AA} & S_{AB}\\ S_{BA} & S_{BB}\end{bmatrix}\begin{bmatrix}E_t^A\\ E_t^B\end{bmatrix}\\ &=[S(AB)]\boldsymbol{E}_t(AB)\end{aligned} \tag{4}$$

The amplitude factor due to path length is omitted in this expression because we are interested in polarimetric information. It is understood in this equation that the target can be regarded as the polarization transformer. The voltage at the receiving antenna is obtained from

$$V=\boldsymbol{h}^T\boldsymbol{E}_s=\boldsymbol{h}(AB)^T[S(AB)]\boldsymbol{E}_t(AB) \tag{5}$$

where $\boldsymbol{h}$ is the polarization state of the receiver when it acts as a transmitter and the subscript T denotes transpose. Therefore the power expression is given as

$$\begin{aligned}P&=|V|^2=|\boldsymbol{h}^T\boldsymbol{E}_s|^2=|\boldsymbol{h}(HV)^T[S(HV)]\boldsymbol{E}_t(HV)|^2\\ &=|\boldsymbol{h}(AB)^T[S(AB)]\boldsymbol{E}_t(AB)|^2\end{aligned} \tag{6}$$

It should be noted that the voltage does not depend on the polarization basis, i.e., the voltage remains the same no matter how the basis is. This invariance leads to the transformation of scattering matrix under the change of polarization basis as follows:
Since the basis transformation matrix $[T]$ using the polarization ratio from the basis (HV) to the new basis (AB) is given by (see Appendix, this $[T]$ is different from the one in Ref. [4])

$$[T]=\frac{1}{\sqrt{1+\rho\rho^*}}\begin{bmatrix}e^{j\phi_1} & \rho^* e^{j\phi_2}\\ \rho e^{j\phi_1} & -e^{j\phi_2}\end{bmatrix}, \tag{7}$$

the vector transformation is carried out as

$$\boldsymbol{E}(AB)=[T]^{-1}\boldsymbol{E}(HV), \text{ or } \boldsymbol{E}(HV)=[T]\boldsymbol{E}(AB), \tag{8}$$

which leads to

$$\begin{aligned}V(HV)&=\boldsymbol{E}_r^T(HV)[S(HV)]\boldsymbol{E}_t(HV)\\ &=\boldsymbol{E}_r(AB)^T([T]^T[S(HV)][T])\boldsymbol{E}_t(AB)\\ &=V(AB).\end{aligned} \tag{9}$$

Therefore the scattering matrix is transformed from the old basis (HV) to the new basis (AB) as

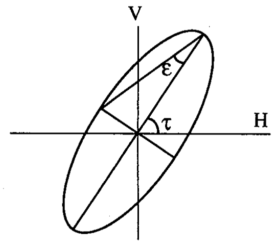

(a) Ellipticity and tilt angles of a polarization ellipse.

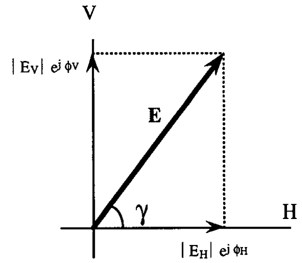

(b) Polarization ratio in the H-V basis.

Fig. 1 Geometric parameters of a polarization ellipse.

$$[S(AB)]=[T]^T[S(HV)][T]=\begin{bmatrix}S_{AA} & S_{AB}\\ S_{BA} & S_{BB}\end{bmatrix}. \tag{10}$$

This transformation indicates that the scattering matrix in any polarization basis can be obtained, provided that the scattering matrix elements in the conventional HV basis are given. The polarization ratio ρ in the HV basis is related to the field vector components and the geometric parameters of the polarization ellipse (see Fig. 1) as

$$\rho=\left|\frac{E_V}{E_H}\right| e^{j(\phi_V-\phi_H)}=\tan\gamma\; e^{j\phi_{HV}} \tag{11a}$$

$$\tan 2\tau=\tan 2\gamma\cos\phi_{HV} \tag{11b}$$

$$\sin 2\varepsilon=\sin 2\gamma\sin\phi_{HV} \tag{11c}$$

where ε and τ are ellipticity angle $(-\pi/4<\varepsilon<\pi/4)$ and tilt angle $(-\pi/2<\tau<\pi/2)$, respectively.

Let's consider the power in the new basis (AB). The unknown is the polarization ratio. It is known [4] that the diagonalization of scattering matrix provides the characteristic polarization state of a radar target. Letting $S_{AB}=0$ in (10) gives, for the monostatic case $S_{AB}=S_{BA}$,

$$\rho S_{VV}+(1-\rho\rho^*)S_{HV}-\rho^* S_{HH}=0. \tag{12}$$

The diagonalization factor, i.e., the polarization ratio in the old basis, is determined to be

$$\rho_{1,2}=\frac{-B\pm\sqrt{B^2-4AC}}{2A} \tag{13}$$

where

$$A=S_{HH}^* S_{HV}+S_{HV}^* S_{VV},\quad B=|S_{HH}|^2-|S_{VV}|^2,$$

$$C=-A^*.$$

Therefore the scattering matrix is in a diagonal form

$$[S(AB)]=\begin{bmatrix} S'_{AA} & 0 \\ 0 & S'_{BB} \end{bmatrix}=\begin{bmatrix} \lambda_1 & 0 \\ 0 & \lambda_2 \end{bmatrix} \tag{14}$$

with

$$\lambda_1=S'_{AA}(\rho_1)=\frac{e^{j2\phi_1}}{1+\rho_1\rho_1^*}(S_{HH}+2\rho_1 S_{HV}+\rho_1^2 S_{VV}) \tag{15}$$

$$\lambda_2=S'_{BB}(\rho_1)=\frac{e^{j2\phi_2}}{1+\rho_1\rho_1^*}(\rho_1^{*2} S_{HH}-2\rho_1^* S_{HV}+S_{VV}) \tag{16}$$

The Co-Pol power in terms of the polarization ratio ρ' in the new basis is given as

$$P_c=|\boldsymbol{E}_t^T[S(AB)]\boldsymbol{E}_t|^2=\left|\frac{[1\ \ \rho']}{1+\rho'\rho'^*}\begin{bmatrix} \lambda_1 & 0 \\ 0 & \lambda_2 \end{bmatrix}\begin{bmatrix} 1 \\ \rho' \end{bmatrix}\right|^2 \tag{17}$$

The Co-Pol means that the receiving antenna has the same polarization state of the transmitter. The maximum of (17), Co-Pol Max, is obtained from $\rho'=0$ in the new basis which gives $P_c=|\lambda_1|^2$. The maximum power thus is derived by the corresponding polarization ratio of ρ_1 in the old basis. On the other hand, Co-Pol null (which gives $P_c=0$), is given by $\rho'=\pm\sqrt{(-\lambda_1/\lambda_2)}$ in the new basis. The same theory and procedure apply to the X-Pol channel power [4].

The above discussion means that the polarimetric imaging in the pixel by pixel basis can be done using the polarization ratio for which we wish to enhance or eliminate a target. That is, if a target scattering matrix in a pixel in a radar scene is extracted, it is possible to calculate the polarization ratio for which the radar channel receives the optimal power. Then, using the polarization ratio, we can calculate the power in the other pixels according to (6). This methodology is the principle of polarimetric imaging in the pixel by pixel basis.

3. Synthetic Aperture FM-CW Radar

In this section, a brief description of synthetic aperture principles for an FM-CW polarimetric imaging is given.

FM-CW radar basically measures a distance between antenna and an object by the beat frequency of a linearly swept transmitted signal and reflected signal from the object. The FM-CW radar utilizes a wideband signal from $f_0-\Delta f/2$ to $f_0+\Delta f/2$ where f_0 is the center frequency. If a point target is located in the Fresnel region (see Fig. 2) and the target reflection coefficient, given by

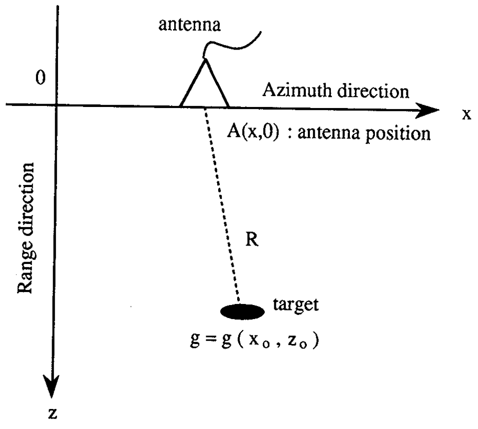

Fig. 2 Positions of antenna and a target.

$$g=g(x_0, z_0) \tag{18}$$

(x_0, z_0): coordinate of the object,

remains the same or at least does not change so much within the swept frequency bandwidth Δf, then the frequency domain beat spectrum due to the target is given by

$$U(x, z)=B\int_0^\infty\int_{-\infty}^\infty f(z-z_0)g(x_0, z_0)h(x-x_0, z_0)\cdot dx_0 dz_0 \tag{19}$$

where

$$f(z-z_0)=\frac{\sin[\alpha(z-z_0)]}{[\alpha(z-z_0)]},\quad \alpha=\frac{2\pi\Delta f}{c},$$

$$h(x-x_0, z_0)=\exp\left[j\,\frac{4\pi f_0}{c}\left\{z_0+\frac{(x-x_0)^2}{2z_0}\right\}\right]. \tag{20}$$

At $z\approx z_0$, Eq. (19) can be modified as

$$U(x, z_0)=B\int_{-\infty}^\infty g(x_0, z_0)h(x_0-x, z_0)dx_0. \tag{21}$$

One can see that this expression is of the convolution integral form and that this expression is equivalent to Fresnel approximation to Kirchhoff-Fresnel diffraction integral equation. We can consider it as one kind of Fresnel hologram. The target reflection function $g(x_0, z_0)$ can be recovered by an inverse convolution integral after multiplying the complex conjugated function h^* by U

$$g(x_0, z_0)=\int_{-\frac{L}{2}}^{\frac{L}{2}} U(x, z_0)h^*(x_0-x, z_0)dx \tag{22}$$

L in Eq. (22) is the antenna-scan width in the azimuth direction, and symbol * denotes complex conjugation. This equation is the basis for the synthetic aperture FM-CW radar principle. It should be noted that (22) gives a single complex value although it is derived from a wideband signal.

The above discussion does not include the polarimetric information. The polarimetric target reflection coefficient can be obtained by a combination of polarimetric measurement. If we measure a target according to (22) making use of HV polarization basis, it is possible to obtain full polarimetric data under the condition that the target scattering characteristics does not depend on the swept frequency band and incidence angle, etc. Since (22) is a complex signal representing a target scattering information, we regard it as an element of a scattering matrix as follows;

$$[S(HV)]=\begin{bmatrix} S_{HH} & S_{HV} \\ S_{VH} & S_{VV} \end{bmatrix}=\begin{bmatrix} g_{HH} & g_{HV} \\ g_{VH} & g_{VV} \end{bmatrix} \tag{23}$$

where the first subscript indicates the polarization state of transmitter and the second subscript represents the receiver polarization. If this (23) is valid, the polarimetric theory in Sect. 2 applies to the FM-CW radar.

4. Experimental Verification

To confirm the applicability of synthetic aperture FM-CW radar polarimetry, a laboratory experiment was carried out to detect a linear target of different orientations with respect to the polarization direction. The target is a metallic pipe of 0.6 cm$\phi \times$100 cm which can be regarded as a linear target. The block diagram of an FM-CW radar system is shown in Fig. 3. In this configuration, transmitting and receiving antennas are separated, which allows one to carry out dual orthogonal channel polarimetric measurement. The separation distance of the antenna is 16.5 cm. The antennas used are standard rectangular horns of precisely the same type operative at 8.2–9.2 GHz. The aperture size is 15.8 cm$\times$11.8 cm. The polarization combination is a set of HH, HV, VH, and VV, where H stands for polarization direction being parallel to the scanning direction (Fig. 4) and V for orthogonal. The radar specifications are listed in Table 1.

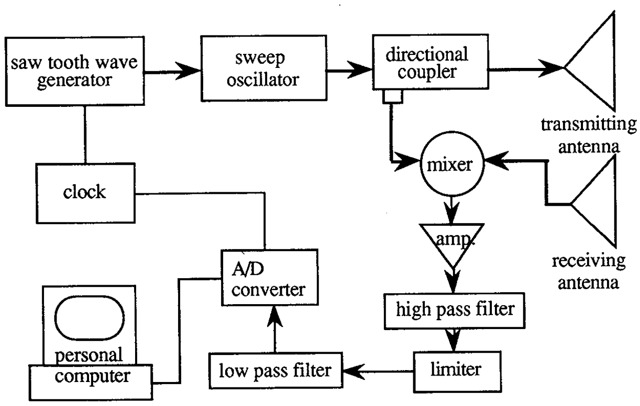

Fig. 3 Block diagram of FM-CW radar.

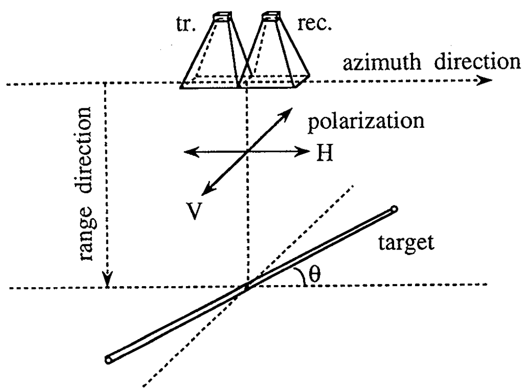

Fig. 4 Measurement scheme.

4.1 Calibration

Since two antennas are used in the system, the radar system is bistatic. On the other hand, the principle of radar polarimetry is derived for the monostatic case. Although two antennas are located very close to each other with the apertures in a common plane looking into the same direction, calibration of the system is crucial to the performance of the system.

Amplitude

The purity of polarization is determined by the X-Pol power level relative to the Co-Pol level. In this radar system, the isolation level between these two channels was found to be less than -30 dB in the operative frequencies. This level was obtained from a reflection measurement using a large flat metallic plate (1 m$\times$1 m) as a calibration target placed at 1.0 meter distance

Table 1 Radar specifications.

RF power	23.5 dBm
Antenna	rectangular horn
Polarization	linear
Sensitivity	-42 dBm
Sweep frequency	8.2 - 9.2 GHz
Sweep time	5.2 msec
Range resolution	1.52 cm
Scanning width	128 cm
Scanning interval	1 cm

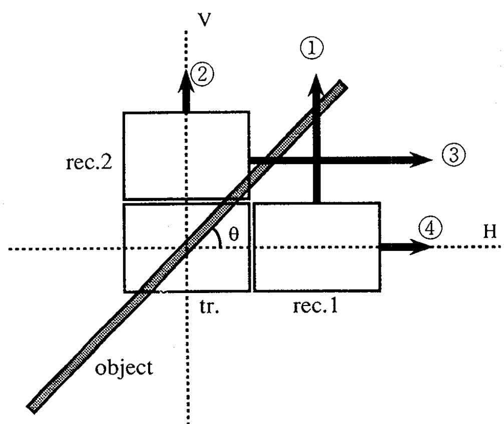

Fig. 5 Phase calibration scheme viewed from top: polarization and target orientation with respect to the scanning direction.

from the radar in an anechoic chamber, and was acceptable to carry out the polarimetric measurement.

Phase

The phase obtained by the system is essentially different from the one in the monostatic radar. To accomodate and calibrate the phase in this system to the monostatic case, we used an extrapolation method. Figure 5 shows the phase calibration scheme, viewed from the antennas (plan view). In the actual situation, the receiving antenna is located in the place of rec. 1 or rec. 2 depending on the polarization with the transmitting antenna fixed at "tr.," for example, rec. 1 for the V-Pol reception and rec. 2 for the H-Pol reception with the V-polarized transmitting antenna. Let's denote the scattering matrix obtained by this bistatic system as

$$[S_{bi}(HV)]=\begin{bmatrix} g_{HH} & g_{HV} \\ g_{VH} & g_{VV} \end{bmatrix}. \qquad (24)$$

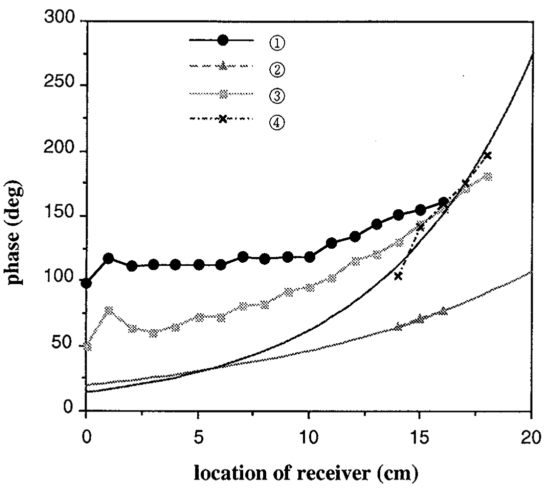

(a) VH

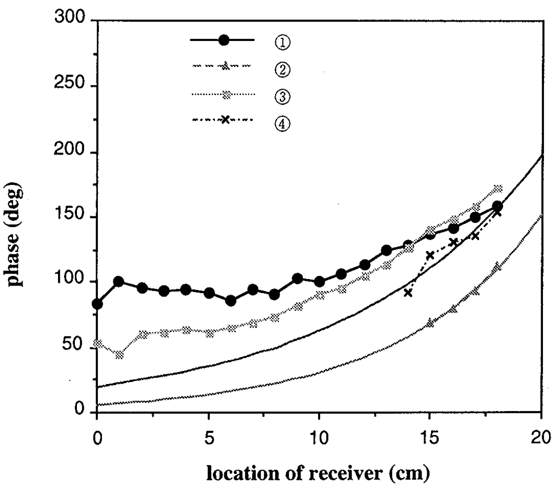

(b) HV

Fig. 6 Phase measured at a 60° oriented pipe (0.6 cm$\phi\times$100 cm).

The matrix elements contain the phase error due to the antenna position. So, we examined the phase change of these elements by moving the receiving antenna from the position of rec. 1 to the direction of 1 and 4, or from the position of rec. 2 to the direction of 2 and 3, at an incremental interval of 1 cm. This procedure was repeated for all polarization combination of HH, HV, VH, and VV. It is now possible to estimate the phase for the monostatic case by the extrapolation technique applied to the measured data. If we let $\Psi_{pq}=\Psi_{mono}-\Psi_{bi}$ as the phase difference between the estimated monostatic case Ψ_{mono} and the bistatic case Ψ_{bi} with the receiving antenna located at the position of rec. 1, the scattering matrix for the monostatic case can be obtained as

$$[S_{mono}(HV)]=\begin{bmatrix} g_{HH}e^{i\Psi_{HH}} & g_{HV}e^{i\Psi_{HV}} \\ g_{VH}e^{i\Psi_{VH}} & g_{VV}e^{i\Psi_{VV}} \end{bmatrix}. \qquad (25)$$

Figure 6 shows one example of the experimental phase measured for a 60° oriented pipe. Although the phases for the bistatic case are different for VH and HV, the estimated monostatic phase by the extrapolation converges to a certain value. We took the averaged phase at 0 cm as the phase Ψ_{mono}. Thus, the phase is calibrated at the place where the transmitting antenna is located at the zenith of the target using the above procedure.

4.2 Polarimetric Detection of Pipe

The same pipe which was employed in the previous section was used as a linear target and was placed 80 cm from the antenna as shown in Fig. 4. The orientation angles are 60° and 45°. The antennas are scanned one-dimensionally at 1 cm incremental interval from 0 up to 127 cm in the azimuth direction. Figure 7 shows the synthetic aperture images for each polarization when the pipe orientation angle is 60°. The power is calculated according to (6) using the uncalibrated scattering matrix, the range is measured from the antenna aperture, and the azimuth direction represents the antenna-scanned direction. It is seen that the image with VV-pol produces the largest power. Using the phase calibration procedure, the scattering matrix for the target was found to be

$$[S(HV)]=\begin{bmatrix} -0.284+j0.339 & -0.046+j0.439 \\ -0.046+j0.439 & -0.417+j0.422 \end{bmatrix} \qquad (26)$$

From this scattering matrix, the Co-Pol channel power can be calculated as a function of geometric parameters of polarization ellipse, which is called "polarimetric signature." The polarimetric response is illustrated in Fig. 8. The Co-Pol max is given by the polarization ratio of $\rho=1.53-j0.14$, which is equivalent to $\tau=57.0°$, $\varepsilon=-2.4°$. This tilt angle corresponds

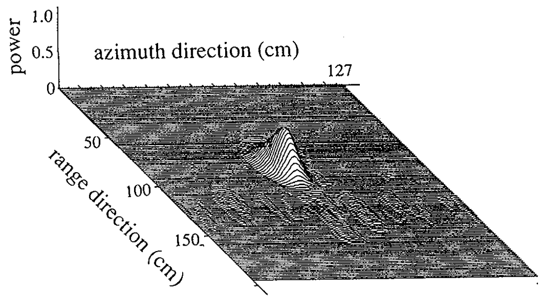

(a) VV

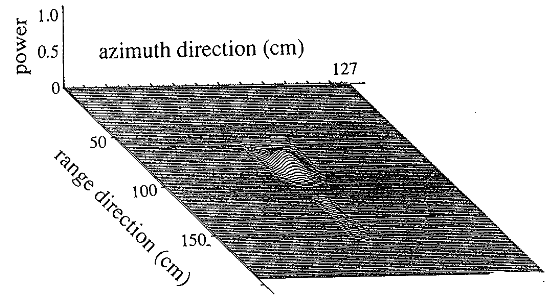

(b) VH

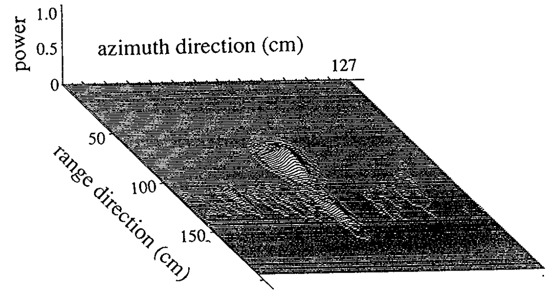

(c) HH

Fig. 7 Detection result of a pipe by *H-V* polarization combination.

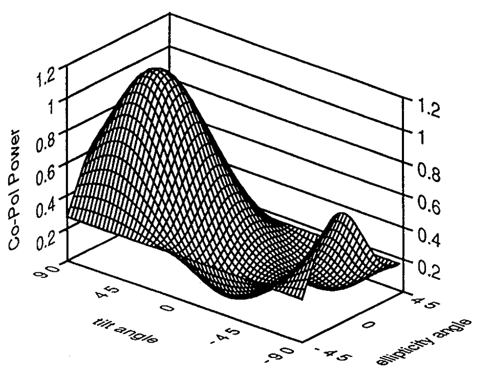

Fig. 8 Polarimetric response of the pipe.

to the orientation angle of the target (60°), and the ellipticity angle indicates the polarization state is almost linear. This fact coincides with the physical experimental situation. On the other hand, Co-Pol null is given by $\rho=0.45-j0.502$. Using these polarization states, the polarimetric images can be synthesized. The resultant Co-Pol max image is displayed in Fig. 9

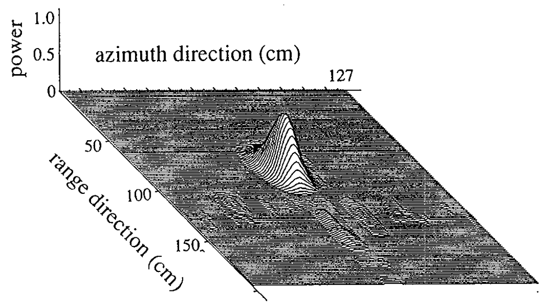

(a) Uncalibrated

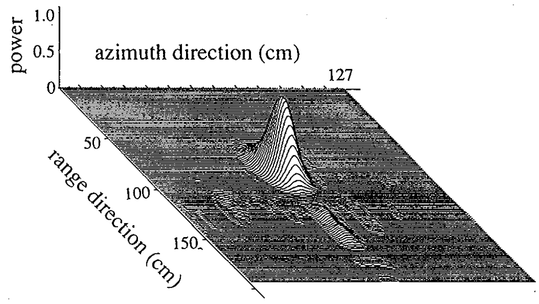

(b) Calibrated

Fig. 9 Co-Pol max image of the pipe.

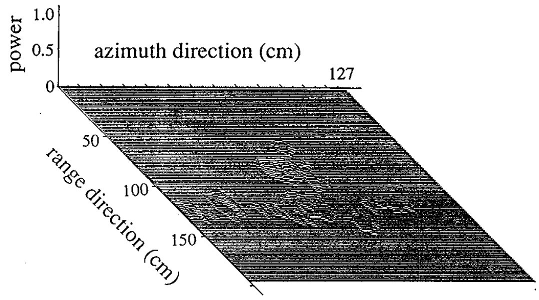

Fig. 10 Co-Pol null image of the pipe (calibrated).

where (a) is derived from the scattering matrix before the phase calibration and (b) is from the calibrated scattering matrix. It is seen that the phase calibration is very important for the precise imaging. Figure 10 shows the Co-Pol null image after the phase calibration. The power is maximized in Fig. 9, wheres it is completely suppressed in Fig. 10, and these images are all different from the fixed polarization images of *HH*, *HV*, or *VV*.

A similar result is obtained for the orientation angle of 45°. The result is omitted to display to save space.

It is understood that the power is enhanced or suppressed by optimal polarization states using the calibrated scattering matrix (26). This fact shows that the radar polarimetry applies to the wideband FM-CW radar and confirms the validity of the replacement of polarimetric target reflection coefficients as the scattering matrix elements.

5. Conclusion

In this paper, we have demonstrated the fundamental result of radar polarimetry applied to the synthetic aperture FM-CW radar. Since the target reflection coefficient obtained by FM-CW radar is complex signal, we regarded it as the scattering matrix element. It is possible to obtain complete scattering matrix element by the polarimetric measurement, which leads to an establishment of full polarimetric FM-CW radar system. The validity was confirmed by a fundamental experiment using a linear target. The phase error due to the bistatic configuration of the experimental radar system is calibrated by the method of extrapolation. The experimental results show that the FM-CW radar polarimetry works well. This polarimetric FM-CW radar seems to have a potential ability in imaging because we can choose any polarization state. Although a fundamental detection result is presented in this paper, practical applications for the two-dimensional mapping or target detection in cluttered environment will be treated in the near future.

Acknowledgement

This work was supported in part by Grant-in-Aid for Scientific Research, Ministry of Education, Japan.

References

[1] Kostinski, A. B. and Boerner, W. M., "On foundation of radar polarimetry," *IEEE Trans. Antennas Propag.*, vol. AP-34, pp. 1359-14-4, 1986.
[2] Giuli, D., "Polarization diversity in radar," *Proc. of the IEEE*, vol. 74, pp. 245-269, 1986.
[3] Van Zyl, J. J., Papas, C. H. and Elach, C., "On the optimum polarization of incoherently reflected waves," *IEEE Trans. Antennas Propag.*, vol. 35, no. 7, pp. 818-825, 1987.
[4] Boerner, W. M., Yan, W. L. A., Xi, A-Q. and Yamaguchi, Y., "On the basic principles of radar polarimetry: the target characteristic polarization state theory of Kennaugh, Huynen's polarization fork concept, and its extension to the partially polarized case," *The Proc. of the IEEE*, vol. 79, no. 10, pp. 1538-1550, Oct. 1991.
[5] Kostinski, A. B., James, B. D. and Boerner, W. M., "Polarimetric matched filter for coherent imaging," *Can. J. Phys.*, 66, pp. 871-877, 1988.
[6] Yamaguchi, Y., Boerner, W. M., Eom, H. J., Sengoku, M., Motooka, S. and Abe, T., "On the characteristic polarization states in the cross-polarized radar channel," *IEEE Trans. Geoscience Remote Sensing*, vol. 30, no. 5, pp. 1078-1080, Sep. 1992.
[7] Boerner, W. M., et al ed., *Direct and Inverse Methods in Radar Polarimetry*, Part 1 and 2, Netherlands, Kluwer Academic Publishers, 1992.
[8] Yamaguchi, Y., Kawakami, A., Mitsumoto, M., Sengoku, M. and Abe, T., "Synthetic aperture FM-CW radar applied to detection of metallic objects," *IEICE Trans.*, vol. J74-B-II, no. 7, pp. 413-420, 1991.
[9] Yamaguchi, Y., Nishikawa, T., Sengoku, M., Boerner, W. M. and Eom, H. J., "On the fundamental study of radar polarimetry in FM-CW radar," *Proc. IEICE Spring Conf.'93*, SB-1-4.
[10] Nishikawa, T., Yamaguchi, Y. and Sengoku, M., "Polarimetric and synthetic aperture FM-CW radar imaging," *IEICE Technical Report*, AP92-98, Nov. 1992.

Appendix: Basis and Vector Transformation Matrices Using Polarization Ratio

In general, a vector $\boldsymbol{w}$ can be expressed in any basis. For example, let $\boldsymbol{w}$ be expressed in the (ab) and in the (xy) basis as

$$\boldsymbol{w}=\alpha_1\boldsymbol{a}+\alpha_2\boldsymbol{b}=\beta_1\boldsymbol{x}+\beta_2\boldsymbol{y} \tag{A·1}$$

where $\boldsymbol{a}$ and $\boldsymbol{b}$ are the new basis vectors, and, $\boldsymbol{x}$ and $\boldsymbol{y}$ are the old basis ones. In a matrix notation, it becomes

$$\boldsymbol{w}=[\boldsymbol{a}, \boldsymbol{b}]\begin{bmatrix}\alpha_1\\ \alpha_2\end{bmatrix}=[\boldsymbol{x}, \boldsymbol{y}]\begin{bmatrix}\beta_1\\ \beta_2\end{bmatrix} \tag{A·2}$$

[ ] represents a 2×2 matrix and ( ) represents a 2×1 vector component in this appendix. The basis vectors can be transformed as

$$[\boldsymbol{a}, \boldsymbol{b}]=[\boldsymbol{x}, \boldsymbol{y}]\begin{bmatrix}a_1 & b_1\\ a_2 & b_2\end{bmatrix}=[\boldsymbol{x}, \boldsymbol{y}][T] \tag{A·3}$$

where $[T]$ is the basis transformation matrix from the old basis (xy) to the new basis (ab) expressed in the basis (xy). On the other hand, the vector component can be transformed from the (xy) basis to the (ab) basis as

$$\begin{bmatrix}\alpha_1\\ \alpha_2\end{bmatrix}=[T]^{-1}\begin{bmatrix}\beta_1\\ \beta_2\end{bmatrix}=[U]\begin{bmatrix}\beta_1\\ \beta_2\end{bmatrix} \tag{A·4}$$

or in an equivalent vector notation,

$$\boldsymbol{w}(ab)=[T]^{-1}\boldsymbol{w}(xy)=[U]\boldsymbol{w}(xy) \tag{A·5}$$

where $[U]=[T]^{-1}$ is the vector transformation matrix, which is different from the one described in Ref. [4]. These transformation matrices are unitary and must satisfy the following conditions,

$$[T]^{-1}=[T]^{*T}=[T]^{\dagger}, \text{ and } |\det[T]|=1 \tag{A·6}$$

where $\dagger$ denotes hermitian conjugate.

Now, consider two orthogonal basis vectors which are expressed in term of the x-y components and the polarization ratio as

$$\boldsymbol{a}(xy)=\begin{bmatrix}a_x\\ a_y\end{bmatrix}=\frac{e^{j\phi_1}}{\sqrt{1+\rho\rho^*}}\begin{bmatrix}1\\ \rho\end{bmatrix},$$
$$\boldsymbol{b}(xy)=\begin{bmatrix}b_x\\ b_y\end{bmatrix}=\frac{e^{j\phi_2}}{\sqrt{1+\rho\rho^*}}\begin{bmatrix}\rho^*\\ -1\end{bmatrix}. \tag{A·7}$$

Therefore the basis transformation matrix $[T]$ and the vector transformation matrix $[U]$ are given as

$$[T]=\frac{1}{\sqrt{1+\rho\rho^*}}\begin{bmatrix} e^{j\phi_1} & \rho^* e^{j\phi_2} \\ \rho e^{j\phi_1} & -e^{j\phi_2} \end{bmatrix}, \qquad (\mathrm{A}\cdot 8)$$

$$[U]=[T]^{-1}=\frac{1}{\sqrt{1+\rho\rho^*}}\begin{bmatrix} e^{-j\phi_1} & \rho^* e^{-j\phi_1} \\ \rho e^{-j\phi_2} & -e^{-j\phi_2} \end{bmatrix}. \qquad (\mathrm{A}\cdot 9)$$

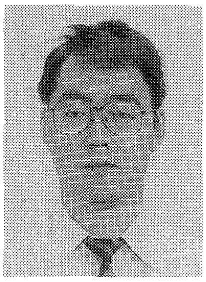

Yoshio Yamaguchi was born in Niigata, Japan, on March 12, 1954. He received the B.E. degree in electronics engineering from Niigata University in 1976, and the M.E. and Dr.Eng. degrees from Tokyo Institute of Technology, Tokyo, Japan, in 1978 and 1983, respectively. In 1978, he joined the Faculty of Engineering, Niigata University, where he is now an Associate Professor. From 1988 to 1989, he was a Research Associate at the University of Illinois at Chicago. His interests are in the field of propagation characteristics of electromagnetic waves in lossy medium, radar polarimetry, microwave remote sensing and imaging. Dr. Yamaguchi is a member of IEEE, and the Japan Society for Snow Engineering.

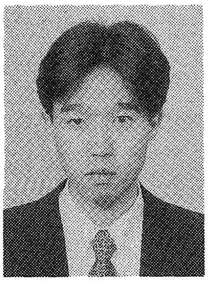

Toru Nishikawa was born on April 25, 1969. He received the B. degree in Information Engineering from Niigata University in 1992. He is engaged in polarimetric radar imaging.

Masakazu Sengoku was born in Nagano Prefecture, Japan, on October 18, 1944. He received the B.E. degree in electrical engineering from Niigata University, Japan, in 1967 and the M.E. and Ph.D. degrees from Hokkaido University in 1969 and 1972, respectively. In 1972, he joined the staff at Hokkaido University as a Research Associate. In 1978, he was an Associate Professor at Niigata University, where he is presently a Professor. During 1986–1987, he was a Visiting Scholar at the University of California, Berkeley, and at the University of Illinois, Chicago. His research interests include transmission of information, network theory, and graph theory. He is a recipient of the best paper award of IEICE in 1992. Dr. Sengoku is a member of Japan Society for Industrial and Applied Mathematics, and IEEE.

Wolfgang-M. Boerner was born on July 26, 1937 in Papua-New Guinea. He received the Arbitur (B.S.) degree from the August on Platen Gymnasium, Ansbach, West Germany in 1958, Dipl. Ing. (M.Sc.) degree from the Technische Universitat Munchen in 1963, and Ph.D. from the University of Pennsylvania, Philadelphia in 1967. From 1967 to 1968 he was a Research Assistant Engineer at the Department of Electrical and Computer Engineering, the University of Michigan. In 1968 he joined the Electrical Engineering Department, University of Manitoba, and in 1978 he joined the Department of Electrical Engineering and Computer Science, University of Illinois at Chicago, where he is a Professor. He is a member of the IEEE, the Canadian Association of Physicists, Sigma XI, the Society of Photo-Optical Instrumentation Engineers, the Optical Society of America, the Society of Exploration Geophysicists, the Society of Engineering Sciences, the American Association for the Advancement of Science, the Fulbright Alumni Association; and he is a member of the U.S. Commissions B, C, and F of the International Scientific Radio Union. He is also a Fellow of the IEEE, of the Humbolt Society for the Advancement of Science of the Federal Republic of Germany and of the Japan Society for the Promotion of Science.

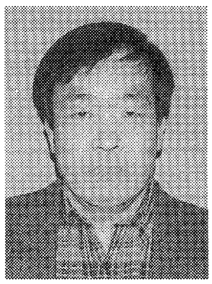

Hyo Joon Eom received the B.S. degree in electronic engineering from Seoul National University, Korea, and M.S. and Ph.D. degrees in electrical engineering from the University of Kansas, Lawrence, in 1977 and 1982, respectively. From 1981 to 1984, he was a research associate at the Remote Sensing Laboratory of the University of Kansas. From 1984 to 1989, he was with the faculty of the Department of Electrical Engineering and Computer Science, University of Illinois at Chicago. He joined the Department of Electrical Engineering, Korea Advanced Institute of Science and Technology in 1989 as an associate professor. His research interests are radar remote sensing and wave scattering.